Photoinduced energy and electron transfer in 1,8-naphthalimide–corrole dyads

Mariusz Tasior,[a] Daniel T. Gryko,*[a] Marek Cembor,[b] Jan S. Jaworski,[b] Barbara Ventura[c] and Lucia Flamigni*[c]

Received (in Durham, UK) 19th September 2006, Accepted 30th November 2006
First published as an Advance Article on the web 20th December 2006
DOI: 10.1039/b613640k

A series of corrole-1,8-naphthalimide dyads has been synthesized. The dyads were assembled in a convergent fashion from two fragments *via* a corrole forming reaction. Central to the success of the synthetic strategy was the preparation of suitably functionalized derivatives of naphthalene-1,8-carboxymide. Six different dyads possessing either a different linker (a *meta*-phenylene or a *para*-phenylmethylene) or a corrole with different substituents at the 5 and 15 positions were prepared. A photophysical and spectroscopic characterization of the dyads and the reference models show that whereas upon selective excitation of the corrole component no photo-induced process occurs, excitation of the naphthalimide unit results in very efficient energy or electron transfer processes. The electron transfer contributes to the quenching process with a ratio between 0% and 85% depending on the nature of the corrole accepting unit. The processes are discussed in the frame of current theories. This is the first report of stable corrole-based dyads with interesting photo-activity at ambient temperature.

Introduction

Photoinduced electron and energy transfer play a key role in light-driven chemical, physical and biological processes. Photosynthesis represents a noteworthy and ubiquitous model that has motivated design of many elaborate assemblies to convert light energy into chemical potential.[1] Although research done in this area has explained many phenomena and answered many questions, unsolved problems provide rationale to search for new systems differing from the previous ones for photoactive unit, linker, spatial arrangement, *etc*.[2] In order to mimic the photosynthetic processes, covalently linked arrays of various chromophores and various complexity are used.[1] Although a great variety of organic and inorganic photoactive unit have been investigated, in this regard porphyrins are still the most often used.[3] Porphyrins almost monopolize the study of photoactive arrays, due to their easy availability and large body of information on their synthetic manipulations[4] and photophysical processes.[5] However many other porphyrinoids have interesting photophysical properties and have been used as photoactive components in the construction of models mimicking various stages of photosynthesis. For example phthalocyanins,[6] subphthalocyanins,[7] chlorins,[8,9] or fused porphyrins,[10] have been successfully used for making photo-active multipartite arrays. Between others corroles—one carbon short analogs of porphyrins-have one additional advantage, since they became easily available after the last developments.[11] Their availability has been steadily increasing since 1999 to challenge the supreme position of porphyrins.[12] Surprisingly, fundamental photophysical behavior of corroles has been rarely studied until recently.[13,14] These aromatic tetrapyrrolic macrocycles exhibit some interesting properties when compared to porphyrins: higher fluorescence quantum yield, larger Stokes shift, no phosphorescence, more intense absorption of red light. Moreover, corroles combine in the same molecule a reasonable ease of oxidation with a reasonable ease of reduction. Stable systems containing corrole linked with other chromophores able to exhibit electron transfer or energy transfer under normal conditions have been unknown until now.[14e,f] Studying corroles offers some additional interesting challenges and opportunities. Attaching corroles to electron acceptors should lead to more stable molecules since the effective electron density on corrole will decrease after excitation and electron transfer. Recently, we started a broad photophysical project aiming to explore the possibilities offered by corroles as part of multicomponent systems.[13] Among many different counterpart chromophores we decided to focus on aromatic imides which can act both as electron acceptor and as energy donor. A variety of porphyrin–aromatic imides-based multicomponent systems bearing four or more donor and acceptor moieties have been reported.[1d,e,3e,15] Aromatic imides have proven useful in dyads and more complex devices; they are chemically very robust and can be linked to other molecules in ways that limit conformational mobility. We have chosen 1,8-napthalimides as the simplest, prototypical example of the aromatic imides family. Derivatives of 1,8-naphthalimide have been extensively studied in recent years owing to their interesting photophysical properties[16] and the wide range of applications.[17]

[a] *Institute of Organic Chemistry of the Polish Academy of Sciences, Kasprzaka 44/52, 01-224 Warsaw, Poland. E-mail: daniel@icho.edu.pl; Fax: +48 22 6326681; Tel: +48 22 3432036*
[b] *Faculty of Chemistry, Warsaw University, Pasteura 1, 02-093 Warsaw, Poland*
[c] *ISOF-CNR, Via P. Gobetti 101, 40129 Bologna, Italy. E-mail: flamigni@isof.cnr.it; Fax: 39 051 6399844; Tel: 39 051 6399812*

They are known to act as electron acceptor,[18a,b] electron donor[18c] or energy donor[18d] in various systems ranging from sensitizers for Grätzel-type solar cells[19a,b] to logic gates,[19c] sensors[19d] and charge separation mimics.[18c] An advantage of 1,8-napthalimides over analogous pyromelitic bisimide, napthalbisimide and perylenebisimide is the simple preparation of the necessary intermediates and the reasonable solubility. In principle 1,8-napthalimides can absorb blue, green, or yellow light by adjusting the substituent at its 4-position.[20] We have chosen unsubstituted 1,8-napthalimides which absorb high-energy photons (λ_{max} = 335 nm) which could be transmitted to the corrole core *via* possible energy transfer.

In this paper we chose three different corroles to couple to the 1,8-napthalimide and varied the oxidation potential of the former by using different substitution patterns. At the same time we changed the linker between the imide component, which plays the role of electron acceptor and energy donor, and the corrole component, acting as electron donor and energy acceptor, in order to change the electronic coupling between the units. Our aim is to exploit the ability of the dyads to act as energy or electron transducer. The results indicate that the energy stored in the excited state of the imide can be efficiently used either to transfer electrons from the corrole to the imide or to transfer energy from the imide to the corrole, and that the relative yield of the processes is tuned by the redox properties of the corrole.

Results and discussion

Design

Several issues merit particular consideration when contemplating the synthesis of complex corrole containing dyads. From the standpoint of synthetic efficiency, in analogy to porphyrins, two general strategies are possible. The first one starts with the synthesis of corrole followed by modifications of peripheral substituents. The second strategy would start with the preparation of an elaborated aldehyde which would then be used in the corrole forming reaction. Given the moderate stability of corroles it is desirable to gain significant relief from the corrole manipulations. In this regard we decided to follow the second route.

We decided to build up on our experience in the synthesis of *meso*-substituted *trans*-A_2B-corroles from dipyrromethanes and aldehydes.[21] This methodology allows to introduce the desired substituent at the 10 position of the macrocycle core. The two remaining identical substituents at the positions 5 and 15 allow the control of other properties of the system like: solubility, stability and redox properties. We envisaged using a few different type of substituents at these positions. As far as the linker connecting both chromophores is concerned we have chosen simple phenylene and phenylmethylene groups which should guarantee a good structural control and a sufficient electronic coupling to allow intramolecular processes.

Synthesis

In the light of the above considerations the crucial part of the dyads' synthesis was the facile generation of the pivotal 1,8-napthalimide core, endowed with an aldehyde functionality for further elaboration. Obviously, synthons for such synthesis had to possess both primary amino and formyl groups, but the latter one has to be present in a protected form. We started our experiments with attempts to synthesize an aldehyde bearing the *para*-phenylene linker. Initially, we thought that the simplest way to prepare the corresponding aldehyde would be starting from anhydride **1** and *para*-toluidine **2**. In analogy to previous results with *N*-phthaloyl-*para*-toluidine[13b] we planned to oxidize methyl group to formyl group in respective imide **5**. This compound was synthesized from anhydride **1** according to a known procedure, however all attempts to oxidize it to the corresponding aldehyde **6** failed regardless of the use of numerous reagents like CAN, IBX, PCC, SeO_2 *etc*. (Scheme 1).

Another option which was considered, started from the respective 4-aminobenzyl alcohol **3**. The corresponding imide would be then an excellent precursor of the aldehyde **6**. Unfortunately, the exposure of alcohol **3** to anhydride **1** in boiling DMF resulted in an intractable mixture which did not contain even traces of the desired product (Scheme 1). The failure in this reaction can be attributed to competitive decomposition of substrate under the reaction conditions. All attempts to perform this process under more gentle conditions failed (Scheme 1).

It is known that commercially available polymer of 4-aminobenzaldehyde **4** reacts with phthalic anhydride to give the respective 4-(*N*-pthaloyl)benzaldehyde in a good yield.[22] The reaction of the polymer of 4-aminobenzaldehyde with anhydride **1** in boiling acetic acid failed to give the desired aldehyde in reasonable yield (Scheme 1).

In the light of these results and due to the fact that the exact structure of the connector was not a crucial objective in this project we turned our attention to an alternative *meta*-phenylene linker. The reaction of 3-aminobenzyl alcohol **7** with anhydride **1** furnished the respective imide **9** in 55% yield. Subsequently, alcohol **9** was oxidized to aldehyde **10** using Dess–Martin periodinate in quantitative yield (Scheme 2). We found that aldehyde **10** can be also obtained directly from polymer of 3-aminobenzaldehyde **8** and anhydride **1** in boiling acetic acid in 90% yield (Scheme 2).

The second important building block—aldehyde **13**—was synthesized from aminoacetal **11** obtained from 4-cyanobenzaldehyde according to literature procedure.[23] This compound

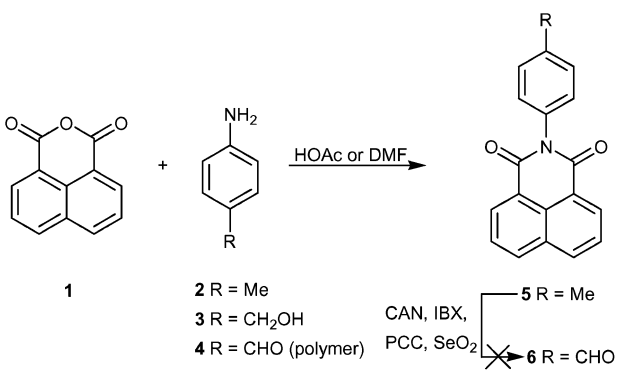

Scheme 1

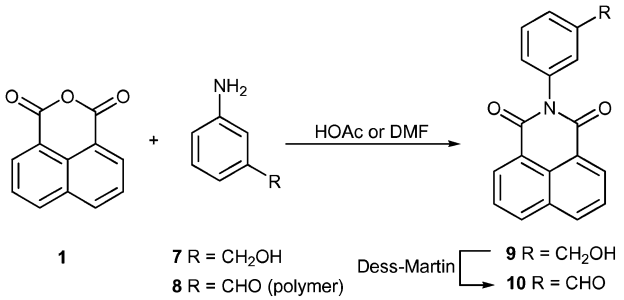

Scheme 2

was found to react with anhydride **1** in boiling EtOH in 100% yield. Subsequent cleavage of the acetal group with a mixture of TFA and H_2SO_4 furnished aldehyde **13** in 95% yield (Scheme 3).

The next stage of our synthesis involved the construction of the corrole ring *via* a [2 + 1] route. This strategy was extensively studied and corroles were prepared from aldehydes **10** and **13** under conditions previously optimized.[21] In order to diversify oxidation potential we decided to use three different dipyrromethanes **14**, **15** and **16**. Among them mesityldipyrromethane **14** is precursor of corroles that is rather easy to oxidize. On the other hand the presence of pentafluorophenyl groups (dipyrromethane **16**) is known to increase significantly the oxidation potential of corroles.[24] Dyads **C1-NI1**, **C1-NI2**, **C1-NI3**, **C2-NI1**, **C2-NI2** and **C2-NI3** were synthesized with yields in the range 6–22% (Scheme 4, Chart 1). Exceptionally low yield was obtained for dyad **C1-NI1**. This result was attributed to low stability of this corrole and to its partial decomposition during purification process. Additional five model compounds, **C1**, **C2**, **C3**, **NI1** and **NI2** (Chart 1), needed for our study were synthesized in analogous way from dipyrromethanes **14**, **15**, **16** and *para*-tolualdehyde or from anhydride **1** and simple primary amines.

Spectroscopic and photophysical properties

A spectroscopic and photophysical investigation was carried out on corrole component models **C1**, **C2**, **C3** and on naphthalene imide component models **NI1** and **NI2** as well as on the six dyads **C1-NI1**, **C2-NI1**, **C3-NI1** and **C1-NI2**, **C2-NI2**, **C3-NI2** reported in Chart 1. The absorption spectrum of imides **NI1** and **NI2** in toluene is nearly identical and displays bands at 333–334 nm (ε = 12 800 M^{-1} cm^{-1}) and 347–349 nm (ε *ca.* 11 400 M^{-1} cm^{-1}), Table 1. Model **C1** displays a splitting of the Soret band which is typical of corroles with *meso* aryl groups bearing a bulky *ortho* substituent[13a] and previously assigned to a deviation from planarity of the macrocycle induced by crowding of substituents.[14b] Also the chlorine substituted corrole model **C2** displays such splitting which is absent in the case of fluorine substituted corrole **C3** (Table 1 and Fig. 1).

The dyads **C1-NI1**, **C2-NI1**, **C3-NI1** and **C1-NI2**, **C2-NI2**, **C3-NI2** display spectra which are essentially the superimposition of the absorption spectra of the component models, Table 1 and Fig. 1. The good additive properties of the spectra points to a rather weak electronic coupling between the components and allows an approach based on a localized description of the individual subunits.

From inspection of the spectra of Fig. 1 one can see that selective excitation of the corrole component in the dyads is possible at wavelength >380 nm, whereas excitation of the imide unit is possible only with a *ca.* 50% ratio (*i.e.* 50% excitation of corrole component and 50% excitation of the imide component) in the range 330–350 nm.

The luminescence spectra of imides **NI1** and **NI2** in toluene upon excitation at 330 nm are shown in Fig. 2 upper panel, both at 295 K and at 77 K in a rigid toluene matrix. There is a very low room temperature luminescence from **NI1**, Φ_{fl} = 7 × 10^{-5}, and a good luminescence from **NI2**, Φ_{fl} = 0.015, λ_{max} at 396 nm, whereas at 77 K intense fluorescence and a weak phosphorescence are detected from both imides.

The luminescence spectra of corrole models in toluene upon excitation at 560 nm are reported in the lower panel of Fig. 2. Their emission yields is variable, Φ_{fl} = 0.22 for **C1**, Φ_{fl} = 0.06 for **C2** and Φ = 0.14 for **C3**, but within values typical for free-base corroles.[13a,14b,d] As observed previously no phosphorescence is observed in any of the examined corroles.[13a]

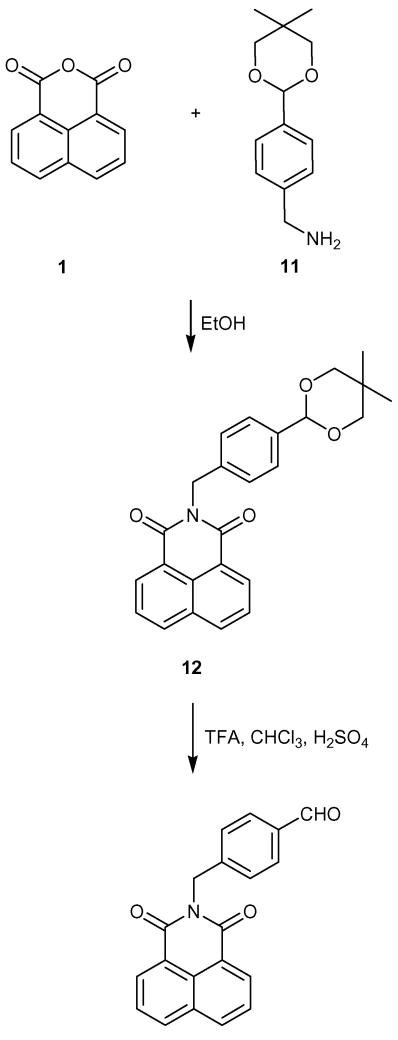

Scheme 3

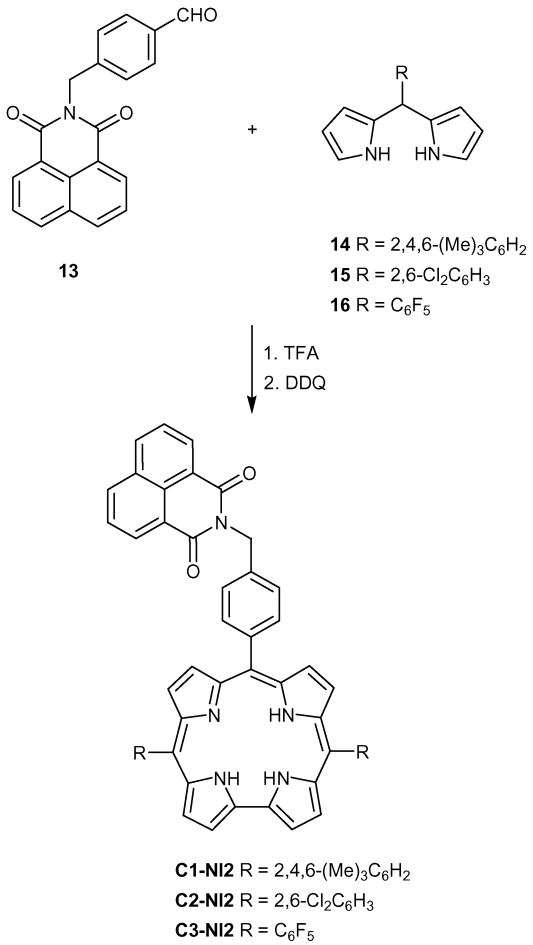

Scheme 4

Time resolved experiments in the pico and nanosecond range in air-equilibrated toluene allow to derive lifetimes of 10 ps for **NI1**, 245 ps for **NI2** and 5.1 ns, 1.7 ns, 3.8 ns for **C1**, **C2** and **C3**, respectively (Table 2). The anomalous behavior of 1,8-naphthalene imide **NI1** with respect to **NI2** and other naphthalene imides,[16a] consisting of an extremely short lifetime and a very weak room temperature luminescence seems to be related to the phenyl substituent at the nitrogen. Similar results were in fact detected from an *N*-phenyl 2,3-naphthalene imide ($\Phi_{fl} < 2 \times 10^{-4}$, $\tau < 50$ ps) and assigned to the formation, in addition to the normal twisted singlet excited state, of a singlet excited state exhibiting co-planarity of the naphthalene and phenyl rings. This state, weakly emitting around 500 nm, is characterized by some charge transfer character and deactivates through rotational or torsional motion of the phenyl substituent.[25] In the present case we do not detect any weak emission around 500 nm, but the interpretation given for the poor luminescence from *N*-phenyl 2,3-naphthalene imide can also satisfactorily explain the very low luminescence yield and lifetime of the present **NI1** chromophore.

The steady state luminescence properties of the dyads were probed upon excitation at 560 nm, where only corrole absorbs and upon excitation at 350 nm, where both imide and corrole moieties absorb 50% of the light. Selective excitation of corrole at 560 nm in the dyads yields emission spectra identical, within experimental error, to those of optically matched solutions of the corresponding corrole, showing that in the dyads no quenching occurs upon excitation of the corroles (Table 2). The results upon excitation of the dyads at 350 nm compared with the models absorbing the same number of photons in the dyads are shown in Fig. 3. In all cases the luminescence localized on the imide **NI2** and **NI1** is totally quenched in the dyads. The quenching of the imide moiety is followed by a poor sensitization of the corrole unit in **C1-NI1** and **C1-NI2** (Fig. 3, upper panel), a significant sensitization of the corrole unit is registered in **C2-NI1** and **C2-NI2** (Fig. 3, middle panel) and a quantitative sensitization is detected in **C3-NI1** and **C3-NI2** (Fig. 3, lower panel), respectively. The data are collected in Table 2. The complete quenching of imide units in the dyads occurs also at 77 K in a toluene glass, data not shown, it is however difficult due to the experimental conditions (see experimental section) to quantitatively assess the sensitization of the corrole unit.

Time resolved luminescence studies with picosecond resolution and 355 nm excitation indicate a lifetime shorter than the instrumental resolution (10 ps) for imide units in the dyads and this points to the occurrence of an efficient quenching of this unit in the array. The quenching rate can be determined from the equation $k = 1/\tau - 1/\tau_0$, where τ and τ_0 are the lifetimes of the quenched unit (*i.e.* in the dyad) and the lifetime of the unquenched unit (*i.e.* in the model), respectively, and results to be $k > 10^{11}$ s^{-1}. On the contrary the lifetime of corrole in the dyads excited both at 355 nm and at 532 nm is essentially identical to that of the model, see Table 2.

Photoinduced processes

In order to discuss the photoinduced processes occurring in the dyads it is convenient to introduce the energy level diagram reporting the energy of the excited states and of the states originating from possible intramolecular reactions, *i.e.* the charge separated (CS) states derived from the transfer of an electron from one component to the other (Fig. 4). The excited state energy levels are derived from the luminescence maxima at 77 K of Table 2. As far as the CS state energy levels are concerned, these can be derived from the energy necessary to reduce the acceptor and to oxidize the donor, *i.e.* from the redox potentials. Both **NI1** and **NI2** are reversibly reduced in benzonitrile at −1.20 V *vs.* SCE by a one-electron process, in line with the literature data on similar aromatic imides and bisimides.[26–30] In the arrays the value was only slightly shifted to more negative values and almost independent of the corrole: −1.23 V for **C1-N1**, **C1-N2, C2-NI1** and **C2-NI2** and −1.22 V and −1.20 V for **C3-NI1** and **C3-NI2**, respectively. Corroles are known to display an irreversible oxidation at potentials which depends on the substitution pattern.[24] The one electron oxidation is followed by fast chemical reactions[24] which shift peak potentials to less positive values. Thus, oxidation peak potentials found should be considered as lower limits of the thermodynamic oxidation potentials. That approximation should be remembered in the following estimation of CS state levels. Oxidation of the present corroles in benzonitrile occurs at 0.58 V for **C1**, at 0.72 V for **C2**, and at 0.86 V for **C3**[24]; these

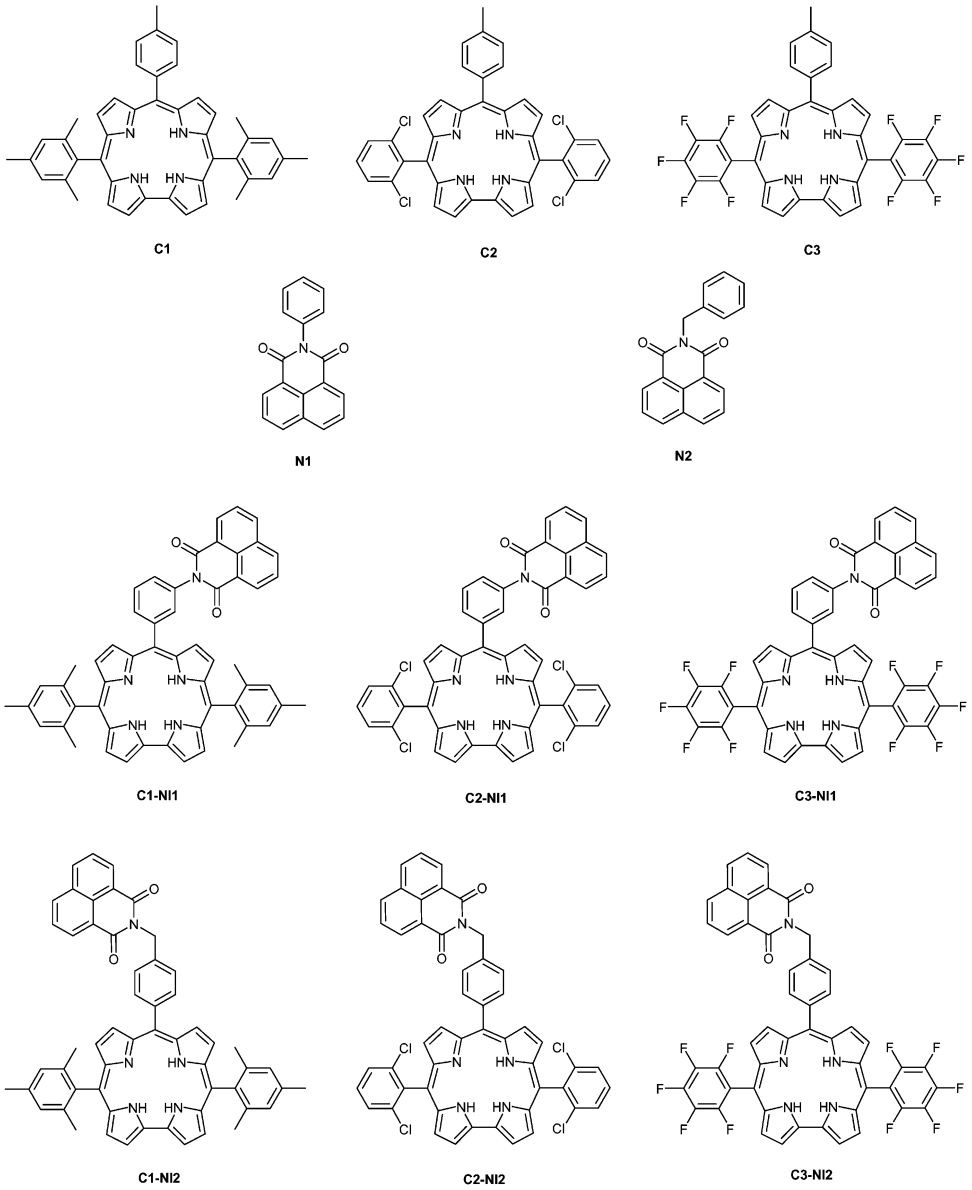

Chart 1 Structures of studied compounds.

data are either unaltered or shifted to slightly more positive values in the array: 0.59 V for **C1-N1** and **C1-N2**, 0.76 V and 0.75 for **C2-NI1** and **C2-NI2** and 0.85 V and 0.84 V for **C3-NI1** and **C3-NI2**, respectively. The small change in the redox processes localized on the units of the arrays compared to the simple models indicate a modest electronic coupling between components of the dyad. The CS state levels in toluene can be estimated after correction for the different solvent used in electrochemistry (benzonitrile). The common correction used to determine the CS state energy level in an apolar solvent from the values of the first oxidation potential of the donor E_{ox} and the first reduction potential of the acceptor E_{red} in a polar solvent takes into account the Coulombic interaction term and the ion solvation energy based on the Born dielectric continuum model according to Weller.[31] This correction tends to overestimate the energy of the charge separated state in those cases when an excited state with charge transfer character is involved in the formation of the CS state, therefore we should have in mind that the derived values can be approximate.[32] The energy of the charge separated states relative to the ground state, ΔG_{CS}, can thus be calculated by the following equation[31]:

$$\Delta G_{CS} = E_{ox} - E_{red} - (14.32/R_{DA}\varepsilon_S) + 14.32\,(1/2r_D + 1/2r_A)\,(1/\varepsilon_S - 1/\varepsilon_P) \quad (1)$$

For the formation of the generic charge separated state C^+–NI^-, involving the transfer of an electron from the corrole to the imide, E_{ox} and E_{red} are the first oxidation potential of the corrole and the first reduction potential of the naphthalene imide in the arrays respectively (see above), $\varepsilon_S = 2.4$ is the dielectric constant of toluene, $\varepsilon_P = 25.9$ is the dielectric constant of benzonitrile. R_{DA}, the center to center donor–acceptor distance is 11.7 Å for the dyads containing **NI2** and 10.4 Å for the dyads containing **NI1** and the

Table 1 Band maxima and molar absorption coefficients for dyads and models in toluene solutions, 295 K

	λ_{max}/nm	$\varepsilon/10^4$ M^{-1} cm^{-1}
NI1	333	1.28
	347	1.12
NI2	334	1.28
	349	1.16
C1	409	12.21
	428	10.16
	568	1.82
	605	1.20
	639	0.71
C1-NI1	333	2.61
	349	2.68
	409	12.59
	428	11.34
	567	1.84
	604	1.24
	638	0.75
C1-NI2	334	2.54
	350	2.71
	409	11.90
	428	10.56
	568	1.65
	605	1.15
	639	0.77
C2	412	12.00
	428	10.67
	563	1.91
	612	1.21
	641	0.70
C2-NI1	334	2.40
	348	2.31
	412	11.72
	428	11.08
	563	1.91
	610	1.21
	641	0.66
C2-NI2	333	2.40
	350	2.33
	413	11.23
	428	10.50
	561	1.81
	611	1.15
	640	0.74
C3	419	12.05
	562	2.03
	617	1.19
	640	0.96
C3-NI1	334	2.34
	349	2.23
	423	11.51
	564	1.81
	616	1.05
	641	0.77
C3-NI2	334	2.31
	350	2.22
	421	11.19
	564	1.71
	618	1.02
	639	0.86

naphthalene imide and corrole radii are r_A = 3.5 Å and r_D = 5 Å, respectively. The results of this calculation yield values of the CS state energy as follows: **C1-NI1** at 2.56 eV, **C1-NI2** at 2.62 eV, **C2-NI1** at 2.73 eV, **C2-NI2** at 2.78 eV, **C3-NI1** at 2.81 eV and **C3-NI2** at 2.84 eV. These can be approximated for C1-NI generic dyads to 2.6 eV, for C2-NI to 2.75 eV and for C3-NI to 2.8 eV and with these values the CS states are reported in Fig. 4.

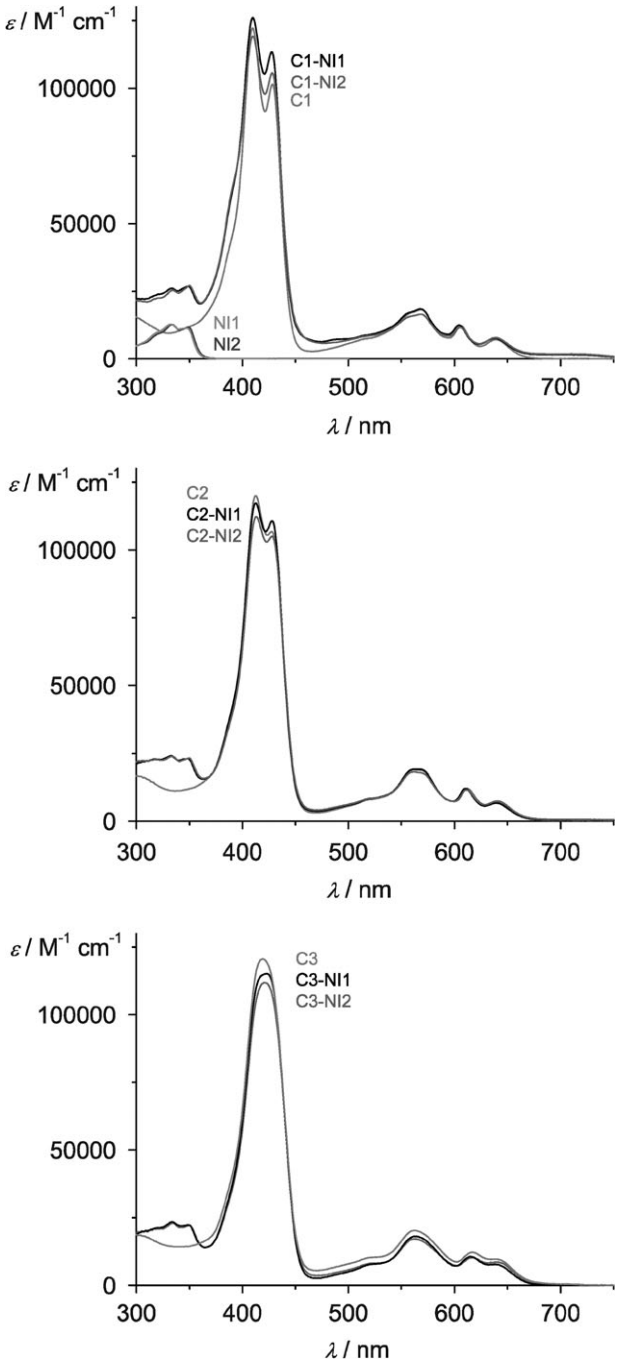

Fig. 1 Absorption spectra of the dyads and the corresponding models in toluene; **NI1** and **NI2** are reported only in the top panel.

Selective excitation of the lowest singlet excited state of the corrole units in the dyads, ^{1}C-NI, does not lead to any photoinduced process and results in the decay of the state as in the isolated molecule, reaction **1**, as testified by the lifetime and emission quantum yield (Table 2). This is quite expected from Fig. 4, which does not show for the generic dyad C-NI any state at lower energy that the singlet localized on corrole ^{1}C-NI.

Excitation at 350 nm leads with a *ca.* 50% ratio to the formation of C-^{1}NI, the singlet excited state localized on

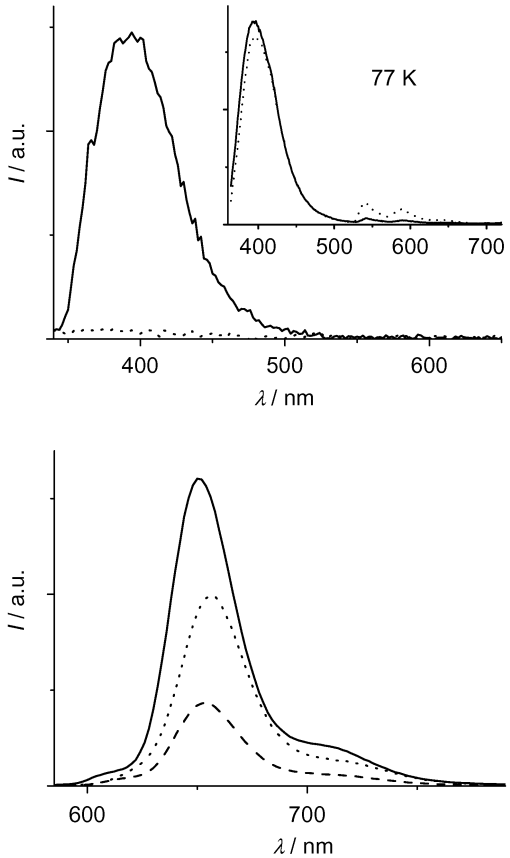

Fig. 2 Luminescence spectra of the models in toluene. Top panel: **NI1** (dot) and **NI2** (solid) excitation at 350 nm ($A = 0.092$) in the inset the 77 K luminescence is reported. Lower panel: **C1** (solid), **C2** (dash) and **C3** (dot), excitation at 560 nm ($A = 0.11$).

naphthalene imide. Energy transfer from this state to the singlet excited state localized on corrole ^{1}C-NI, reaction **2**, is thermodynamically allowed ($\Delta G^0 = -1.2$ eV) and can therefore take place. Accordingly, the lifetime of C-^{1}NI is <10 ps, indicating a quenching with a rate constant $k_{en} > 10^{11}$ s^{-1}. The efficiency of energy transfer to the corrole can be calculated from the relative increase in the emission quantum yield of the corrole unit in passing from selective excitation at 560 nm to excitation at 350 nm, provided one compares cases where the same amount of photons is absorbed by the corrole unit in the dyad and in the reference model. This efficiency is unity (Table 2, Fig. 3) only for the dyads containing the corrole **C3**, **C3-NI1** and **C3-NI2** whereas the efficiency is *ca.* 65% for the dyads containing the corrole **C2**, **C2-NI1** and **C2-NI2**, and is only *ca.* 15% in the case of the dyads containing **C1**, **C1-NI1** and **C1-NI2**. The energy transfer efficiency decreases in the order **C3-NI** > **C2-NI** > **C3-NI** which is the same order exhibited by the oxidation potentials of corroles and is in the reverse order with respect to the energy level of the CS state, see Fig. 4. This leads us to conclude that the decrease in energy transfer efficiency has to be assigned to a competition with an electron transfer reaction which occurs in the excited state C-^{1}NI from the HOMO of the corrole to the HOMO of the naphthalene imide (Fig. 4, reaction **3**), leading to the generic charge separated state C^+-NI^-. Reaction **3** is totally inefficient in the dyads containing corrole **C3**, a $\Delta G^0 \leq -0.3$ eV for electron transfer is probably insufficient to provide a rate able to compete with the rapid energy transfer (Fig. 4, reaction **2**). In the case of dyads **C2-NI1** and **C2-NI2**, characterized by a ΔG^0 of *ca.* -0.35 eV, electron transfer starts to compete (15%) with energy transfer and finally becomes predominant (85%) for dyads **C1-NI1** and **C1-NI2** where the electron transfer reaction has a ΔG^0 of *ca.* -0.5 eV. It should be noticed that in spite of the difference in luminescence

Table 2 Luminescence data of dyads and models in air-equilibrated toluene at 298 K and in rigid toluene glass at 77 K

	295 K					77 K	
	State	λ_{max}/nm	Φ_{fl}[a]	Φ_{fl}[b]	τ/ns[c]	λ_{max}/nm	E/eV[d]
NI1	^{1}NI1	*ca.* 376	—	0.00007	0.010	396	3.13
	^{3}NI1	—	—	—	—	541	2.29
NI2	^{1}NI2	390	—	0.015	0.245	394	3.15
	^{3}NI2	—	—	—	—	542	2.29
C1	^{1}C1	650	0.22	0.22	5.1	644	1.93
C1-NI1	^{1}C1-NI1	650	0.21	0.26	5.0	647	1.92
	C1-^{1}NI1	—	—	<0.00005	< 0.010	—	—
C1-NI2	^{1}C1-NI2	650	0.21	0.24	5.0	649	1.91
	C1-^{1}NI2	—	—	<0.00005	< 0.010	—	—
C2	^{1}C2	653	0.06	0.06	1.7	652	1.90
C2-NI1	^{1}C2-NI1	654	0.06	0.10	1.7	652	1.90
	C2-^{1}NI1	—	—	<0.00005	< 0.010	—	—
C2-NI2	^{1}C2-NI2	653	0.06	0.10	1.7	652	1.90
	C2-^{1}NI2	—	—	<0.00005	< 0.010	—	—
C3	^{1}C3	656	0.14	0.14	3.8	654	1.90
C3-NI1	^{1}C3-NI1	656	0.14	0.29	3.9	655	1.89
	C3-^{1}NI1	—	—	<0.00005	< 0.010	—	—
C3-NI2	^{1}C3-NI2	656	0.13	0.28	3.7	651	1.90
	C3-^{1}NI2	—	—	<0.00005	≤ 0.010	—	—

[a] Luminescence quantum yields in air-equilibrated solutions, excitation at 560 nm. For the standard used see Experimental Section. [b] Luminescence quantum yields upon excitation at 350 nm. The yield is calculated by taking into account the photons absorbed by unit of interest, either corrol or imide, only. For the standard used see Experimental Section. [c] Lifetimes detected after excitation at 355 nm for imides and at 560 nm for corroles. [d] Excited states energy levels derived from the luminescence maxima at 77 K.

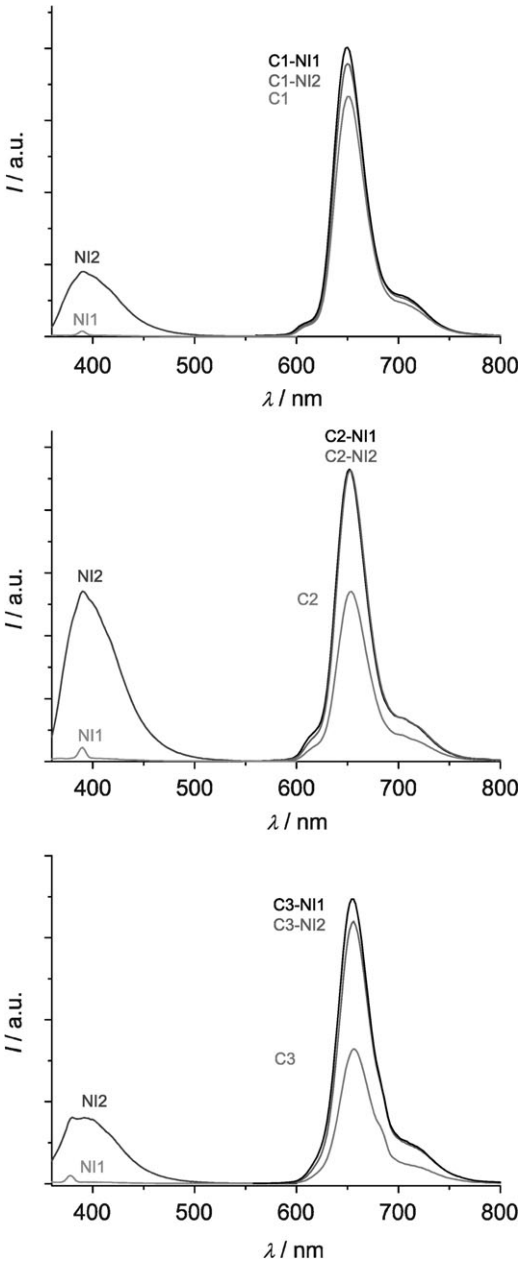

Fig. 3 Luminescence spectra of imides, corroles and dyads in toluene, excitation at 350 nm, $A = 0.1$ for corroles and imides and $A = 0.2$ for dyads. At 350 nm the absorbance is 50% on corrole and 50% on imide component.

properties of the imide **NI1** compared to **NI2**, the photoinduced processes generated in the dyads from the excited states localized on the two imides, either C-^{1}NI1 and C-^{1}NI2, are very similar.

This seems to suggest that the excited state ^{1}NI1, though not emissive, has sufficient lifetime to participate in the intramolecular processes and has an energy level similar to ^{1}NI2. The latter fact is important to determine the driving force and hence the rate of the ensuing reactions. Any attempt to detect the charge separated states C1$^+$-NI1$^-$ and C1$^+$-NI2$^-$ was strongly biased by the spectral features of the reduced acceptor and of the oxidized donor. In fact, the absorbance of the

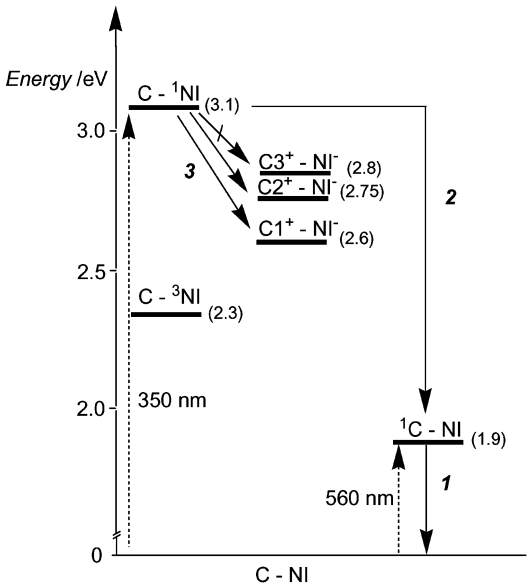

Fig. 4 Energy level diagram for a generic dyad containing naphthalene imide and corrole, **C-NI**. When differences occur in the energy levels the components are specified as C1, C2 or C3.

reduced imide has a maximum at *ca.* 400 nm,[30] out of the wavelength range probed by the experimental set-up used, and the absorption of corrole cations in the visible and near IR region[24] is not high enough to allow a clear differentiation from the absorption spectra of the singlet excited state absorbing in the same spectral region.[13a] We were therefore unable to clearly detect the charge separated states. It is worth noticing that **C1-NI1** and **C1-NI2** displayed, at variance with the other dyads, some slight instability under the extreme laser peak power conditions (GW) used in the picosecond pump and probe experiments. No instability was shown by these and other dyads in all other experiments, confirming the remarkable stability of these compounds.

In order to shed light on the energy transfer process **2**, we discuss the rate k_{en} in the frame of the current theories. Energy transfer between singlet states can occur by two different mechanisms, the Förster mechanism (or dipole–dipole interaction)[33] or the Dexter mechanism (or electron exchange).[34] In case of energy transfer between singlet states with high absorbance and emission quantum yield the dipole–dipole mechanism, in general, prevails whereas for poorly emitting donor or absorbing acceptors the Dexter mechanism, based on the concomitant exchange of two electrons, can prevail. For the dipole–dipole mechanism it is possible to calculate the rate k_{en}^F by means of the following equation:[44]

$$k_{en}^F = \frac{8.8 \times 10^{-25} \kappa^2 \Phi}{n^4 \tau R_{DA}^6} J^F \qquad (2)$$

in which Φ and τ are the emission quantum yield (0.015 for **NI2** and 7×10^{-5} for **NI1**) and the lifetime (245 ps and 10 ps for **NI2** and **NI1**, respectively) of the donor, R_{DA} is the donor–acceptor center-to-center distance (11.7 Å for **NI2** and 10.4 Å for **NI1**), n is the refractive index of toluene and J^F is the overlap integral. κ^2, the orientation factor, takes into

account the relative orientation of the transition dipole moments of the donor and the acceptor and can be simplified to the statistical value, 2/3. J^F, the Förster overlap integral, is calculated from the overlap between the luminescence spectrum of the donor **NI2** and **NI1**, $F(\bar{\upsilon})$ (cm^{-1} units), and the absorption spectrum $\varepsilon(\bar{\upsilon})$ of the acceptors **C1**, **C2** and **C3** (cm^{-1} units), according to eqn. (3).[33]

$$J^F = \frac{\int F(\bar{\upsilon})\varepsilon(\bar{\upsilon})/\bar{\upsilon}^4 d\bar{\upsilon}}{\int F(\bar{\upsilon}) d\bar{\upsilon}} \quad (3)$$

From the experimental emission and absorption spectra, an overlap integral $J^F = 1.46 \times 10^{-13}$ cm^3 M^{-1}, $J^F = 1.47 \times 10^{-13}$ cm^3 M^{-1}, $J^F = 1.50 \times 10^{-13}$ cm^3 M^{-1} is calculated for dyads **C1-NI2**, **C2-NI2** and **C3-NI2**, respectively, whereas a $J^F = 1.04 \times 10^{-13}$ cm^3 M^{-1}, $J^F = 1.07 \times 10^{-13}$ cm^3 M^{-1}, $J^F = 1.14 \times 10^{-13}$ cm^3 M^{-1} is calculated for dyads **C1-NI1**, **C2-NI1** and **C3-NI1**, respectively. From eqn. (2) a rate of energy transfer $k_{en}^F = 3.5 \times 10^{11}$ s^{-1} is derived for the dyads containing NI2 and a $k_{en}^F = 7 \times 10^{10}$ s^{-1} is calculated for the dyads **C1-NI1**, **C2-NI1**, **C3-NI1**. The calculated rates are consistent with the experimental results for the series **C1-NI2**, **C2-NI2**, **C3-NI2**, therefore the mechanism *could* be ascribed to a dipole–dipole interaction. However, given the uncertainty in the experimental rate constant we cannot exclude some contribution by a Dexter-type mechanism. On the contrary the rate calculated according to a Forster mechanism *is not* in agreement with the experimental data ($k_{en} > 10^{11}$ s^{-1}) for the **NI1**-containing compounds. We have therefore to assume for the **NI1** containing series the contribution by an electron exchange mechanism in order to explain the results. Within this mechanism, an electron moves from the half filled LUMO of the imide unit to the empty LUMO of the corrole unit while another electron moves from the filled HOMO localized on the corrole to the half filled HOMO localized on the imide. For this mechanism the energy transfer rate can be expressed in classical terms by the following expression:[34]

$$k_{en}^D = \frac{4\pi^2 H^2}{h} J^D \quad (4)$$

Where H is the intercomponent electronic interaction and J^D is the Dexter overlap integral:

$$J_D = \frac{\int F(\bar{\upsilon})\varepsilon(\bar{\upsilon}) d\bar{\upsilon}}{\int F(\bar{\upsilon}) d\bar{\upsilon} \int \varepsilon(\bar{\upsilon}) d\bar{\upsilon}} \quad (5)$$

J^D calculated from the spectroscopic data is of the order of 10^{-4} cm for all **N1** based dyads. By replacing in eqn. (4) this value and a k_{en}^D of 10^{11} s^{-1}, a value of H of the order of 30 cm^{-1} can be derived. This is a moderate electronic coupling compatible with the compact structure of the **NI1** based dyads, where the two chromophores are essentially in contact, and while sufficient to provide a large electron exchange contribution to the energy transfer process, it would be insufficient to noticeably perturb the spectroscopic and electrochemical properties, in agreement with the experimental observations.

Experimental section

Synthesis

All chemicals were used as received unless otherwise noted. Reagent grade solvents (CH_2Cl_2, hexanes, cyclohexane) were distilled prior to use. All reported ^1H NMR and ^{13}C NMR spectra were recorded on Bruker AM 500 MHz or Varian 400 MHz spectrometers. Chemical shifts (δ ppm) were determined with TMS as the internal reference; J values are given in Hz. UV-Vis spectra were recorded in toluene (Cary). Chromatography was performed on silica (Kieselgel 60, 200–400 mesh), or dry column vacuum chromatography (DCVC)[35] was performed on preparative thin layer chromatography silica (Merck 107747). Mass spectra were obtained *via* EI or electrospray MS (ESI-MS). The purity of all new corroles was established based on ^1H NMR spectra and elemental analysis. The following molecules were prepared according to literature procedures: **5**,[36] **11**,[23] **14**,[37] **15**,[12a,37] **16**,[37] **C3**,[21d] **NI1**[38] and **NI2**.[39]

***N*-[3-(Hydroxymethyl)phenyl)]-1,8-naphthalimide (9).** 1,8-Naphthalic anhydride (3.96 g, 20 mmol) and amine **7** (2.26 g, 20 mmol) were dissolved in DMF (100 mL). The resulting mixture was refluxed for 6 h, then it was cooled down and water (100 mL) was added. The white precipitate was filtered off, washed with cold EtOH and chromatographed (silica, CH_2Cl_2 + 2% MeOH) to afford pure imide **9** (3.3 g, 55%). mp 177–178 °C; ^1H NMR (500 MHz; $CDCl_3$; Me_4Si) 2.00 (br s, 1H, OH), 4.76 (s, 2H, CH_2), 7.24 (m, 1H, C_6H_4), 7.33 (m, 1H, C_6H_4), 7.46–7.49 (m, 1H, C_6H_4), 7.54 (t, 1H, J = 7.7 Hz, C_6H_4), 7.78 (dd, 2H, $C_{10}H_6$), 8.26 (dd, 2H, $C_{10}H_6$), 8.63 (dd, 2H, $C_{10}H_6$); ^{13}C NMR (125 MHz; $CDCl_3$; Me_4Si) δ 64.8, 122.8, 127.00, 127.02, 127.15, 128.5, 129.5, 131.6, 131.7, 134.3, 135.6, 142.6, 164.3; EI-HR obsd 303.0909 [$M^{\bullet+}$], calc. exact mass 303.0895 ($C_{19}H_{13}NO_3$). Anal. calc. for $C_{19}H_{13}NO_3$: C, 75.24; H, 4.32; N, 4.62. Found: C, 75.22; H, 4.12; N, 4.60%; IR (KBr): 781, 1242, 1357, 1377, 1588, 1659, 1706, 3445, 3506.

***N*-(3-Formylphenyl)-1,8-naphthalimide (10).** Alcohol **9** (3.3 g, 11 mmol) was dissolved in CH_2Cl_2 (200 mL) followed by Dess–Martin periodinate (5.03 g, 11 mmol). After stirring for 15 min $Na_2S_2O_3$ (12 g) dissolved in sat. solution of $NaHCO_3$ (50 mL) was added, and resulting suspension was stirred for 30 min until both phases were clear. Subsequently the organic phase was separated, washed with $NaHCO_3$ (50 mL) and water (50 mL), dried with Na_2SO_4 and evaporated. The pure aldehyde was obtained after crystallization ($CHCl_3$–hexane), 2.85 g, 95%. mp 210–212 °C; ^1H NMR (500 MHz; $CDCl_3$; Me_4Si) 7.59–7.63 (m, 1H, C_6H_4), 7.72 (t, 1H, J = 7.8 Hz, C_6H_4), 7.78–7.83 (m, 2H, $C_{10}H_6$), 7.87 (t, 1H, J = 1.9 Hz, C_6H_4), 8.01 (dt, 2H, C_6H_4), 8.29 (dd, 2H, $C_{10}H_6$), 8.65 (dd, 2H, $C_{10}H_6$), 10.07 (s, 1H, CHO); ^{13}C NMR (125 MHz; $CDCl_3$; Me_4Si) δ 122.5, 127.1, 128.5, 129.7, 130.0, 131.8, 134.6, 134.8, 136.3, 137.6, 164.1, 191.1; EI-HR obsd 301.0732 [$M^{\bullet+}$], calc. exact mass 301.0739 ($C_{19}H_{11}NO_3$). Anal. calc. for $C_{19}H_{11}NO_3$: C, 75.74; H, 3.68; N, 4.65. Found: C, 75.50; H, 3.70; N, 4.57%; IR (KBr): 779, 1239, 1356, 1376, 1588, 1664, 1705.

***N*-[4-(5,5-Dimethyl-1,3-dioxan-2-yl)benzyl]-1,8-naphthalimide (12).** 1,8-Naphthalic anhydride (3.96 g, 20 mmol) and acetal

11 (5.3 g, 24 mmol) were suspended in EtOH (100 mL). The resulting mixture was refluxed for 6 h and cooled down. The white precipitate was filtered off and washed with EtOH to afford pure imide (8.0 g, 100%). mp 256–257 °C (EtOH), ^{1}H NMR (500 MHz; $CDCl_3$; Me_4Si) δ 0.77 (s, 3H, CH_3), 1.24 (s, 3H, CH_3), 3.60 (d, 10.5 Hz, 2H, CH_2O), 3.72 (d, 10.5 Hz, 2H, CH_2O), 5.34 (s, 1H, CH), 5.38 (s, 2H, CH_2), 7.44, 7.57 (AA′BB′, J = 8.5 Hz, 2 × 2H, C_6H_4), 7.72 (t, 2H, J = 8 Hz, $C_{10}H_6$), 8.18 (d, 2H, J = 8 Hz, $C_{10}H_6$), 8.58 (d, 2H, J = 8 Hz, $C_{10}H_6$); ^{13}C NMR (125 MHz; $CDCl_3$; Me_4Si) δ 21.9, 23.0, 30.2, 43.3, 77.6, 101.4, 122.7, 126.2, 126.9, 128.1, 129.1, 131.3, 131.6, 134.0, 137.8, 137.8, 164.1; EI-HR obsd 401.1644 [$M^{\bullet+}$], calc. exact mass 401.1627 ($C_{25}H_{23}NO_4$). Anal. calc. for $C_{25}H_{23}NO_4$: C, 74.79; H, 5.77; N, 3.49. Found: C, 74.66; H, 5.52; N, 3.37%; IR (KBr): 774, 1101, 1235, 1336, 1383, 1656, 1699, 2950.

***N*-(4-Formylbenzyl)naphthalimide (13).** Acetal **12** (8.0 g, 2 mmol) was dissolved in CH_2Cl_2 (100 mL), then TFA was added (50 mL) followed by 5% aq H_2SO_4 (25 mL) and the whole mixture was vigorously stirred over night at rt. The flask was placed in an ice-water bath, both acids were neutralized with diluted NaOH solution, and the resulting suspension was extracted with CH_2Cl_2. The organic extracts were evaporated and residue was crystallized from $CHCl_3$ to obtain the title compound as off-white crystals (6.3 g, 100%) which were pure enough for the next step. The pure sample was obtained after flash chromatography (silica, CH_2Cl_2) and crystallization ($CHCl_3$). mp 185–186 °C; ^{1}H NMR (500 MHz; $CDCl_3$; Me_4Si) 5.44 (s, 1H, CH), 7.67, 7.82 (AA′BB′, J = 8 Hz, 2 × 2H, C_6H_4), 7.76 (dd, 2H, $C_{10}H_6$), 8.22 (dd, 2H, $C_{10}H_6$), 8.61 (dd, 2H, $C_{10}H_6$), 9.96 (s, 1H, CHO); ^{13}C NMR (125 MHz; $CDCl_3$; Me_4Si) δ 43.4, 122.4, 127.0, 128.2, 129.2, 129.9, 131.5, 131.6, 134.3, 135.6, 144.1, 164.1, 191.8; EI-HR obsd 315.0883 [$M^{\bullet+}$], calc. exact mass 315.0895 ($C_{20}H_{13}NO_3$). Anal. calc. for $C_{25}H_{23}NO_4$: C, 76.18; H, 4.16; N, 4.44. Found: C, 76.29; H, 4.13; N, 4.43%; IR (KBr): 771, 785, 1339, 1383, 1657, 1695.

10-[(Benz[*de*]isoquinoline-1,3-dion-2-yl)-methyl-*para*-phenyl]-5,15-bis(mesityl)corrole (C1-NI2). Mesityldipyrromethane (**14**) (1.06 g, 4.0 mmol) and aldehyde **13** (630 mg, 2.0 mmol) were dissolved in CH_2Cl_2 (30 mL). Then TFA (3 μL, 0.04 mmol) was added and mixture was stirred at rt for 7 h. *para*-Chloranil (1.47 g, 6.0 mmol) was added and stirring was continued for 16 h. The reaction mixture was concentrated to 1/4 of initial volume and filtered through silica pad (CH_2Cl_2–hexanes, 3 : 1). The fluorescent band was collected, and was chromatographed (DCVC, silica, CH_2Cl_2–hexanes, 1 : 1, then 3 : 1). After evaporation it was crystallized from $CHCl_3$–MeOH to afford pure corrole (262 mg, 16%). R_f = 0.48 (CH_2Cl_2–hexanes, 3 : 1). ^{1}H NMR (500 MHz; $CDCl_3$; Me_4Si) δ (−3)–(−1.5) (br s, 3H), 1.89 (s, 12H, *o*-CH_3 Mes), 2.57 (s, 6H, *p*-CH_3 Mes), 5.67 (s, 2H, CH_2), 7.23 (s, 4H, Mes), 7.79 (dd, 2H, $C_{10}H_6$), 7.87, 8.08 (AA′BB′, J = 8 Hz, 2 × 2H, C_6H_4), 8.23 (dd, 2H, $C_{10}H_6$), 8.28 (d, J = 4 Hz, 2H, β-H), 8.42 (d, J = 4.5 Hz, 2H, β-H), 8.46 (d, J = 4.5 Hz, 2H, β-H), 8.70 (dd, 2H, $C_{10}H_6$), 8.85 (d, J = 4 Hz, 2H, β-H). ESI-HR obsd 820.3677 [M + H^+], calc. exact mass 820.3646 ($C_{56}H_{46}N_4O_2$); Anal. calc. for $C_{56}H_{45}N_4O_2 \cdot H_2O$: C, 80.26; H, 5.65; N, 8.36. Found: C, 80.63; H, 5.43; N, 8.41%. λ_{abs} (toluene, $\varepsilon \times 10^3$) 409 (119), 428 (106), 568 (16.5), 605 (11.5), 639 (7.7) nm.

10-[(Benz[*de*]isoquinoline-1,3-dion-2-yl)-methyl-*para*-phenyl]-5,15-bis(2,6-dichlorophenyl)corrole (C2-NI2). The title compound was synthesized according to the procedure described for **C1-NI2**, starting from 2,6-dichlorophenyldipyrromethane (**15**) (1.16 g, 4.0 mmol) and aldehyde **13** (630 mg, 2.0 mmol). The reaction mixture was concentrated, filtered through silica pad (CH_2Cl_2) and evaporated. The residue was chromatographed (DCVC, silica, CH_2Cl_2–hexanes, 1 : 1, then 3 : 1), evaporated and crystallized ($CHCl_3$–MeOH) to afford pure corrole (300 mg, 17%). R_f = 0.45 (CH_2Cl_2–hexanes, 3 : 1). ^{1}H NMR (500 MHz; $CDCl_3$; Me_4Si) δ (−3)–(−1.5) (br s, 3H, NH), 5.70 (s, 2H, CH_2), 7.63 (t, 2H, 8 Hz, $C_6H_3Cl_2$), 7.75 (d, 8 Hz, 4H, $C_6H_3Cl_2$), 7.82 (t, 2H, J = 8 Hz, $C_{10}H_6$), 7.90, 8.11 (AA′BB′, J = 8 Hz, 2 × 2H, C_6H_4), 8.25 (d, 2H, J = 8 Hz, $C_{10}H_6$), 8.39 (d, J = 4 Hz, 2H, β-H), 8.47 (d, J = 4.5 Hz, 2H, β-H), 8.57 (d, J = 4.5 Hz, 2H, β-H), 8.75 (d, 2H, J = 8 Hz, $C_{10}H_6$), 8.97 (d, J = 4 Hz, 2H, β-H). ESI-LR obsd 872.1 [M + H^+] ($C_{50}H_{30}N_5Cl_4O_2$); Anal. calc. for $C_{50}H_{29}N_5Cl_4O_2$: C, 68.74; H, 3.35; N, 8.02. Found: C, 68.59; H, 3.12; N, 7.94. λ_{abs} (toluene, $\varepsilon \times 10^3$) 413 (112), 428 (105), 561 (18.1), 611 (11.5), 640 (7.4) nm.

10-[(Benz[*de*]isoquinoline-1,3-dion-2-yl)-methyl-*para*-phenyl]-5,15-bis(pentafluorophenyl)corrole (C3-NI2). Pentafluorophenyldipyrromethane (**16**) (1.25 g, 4 mmol) and aldehyde **13** (630 mg, 2 mmol) were dissolved in CH_2Cl_2 (30 mL). Then TFA (30 μL, 0.4 mmol) was added and mixture was stirred at rt for 20 min. The reaction was quenched with the addition of Et_3N (54 μL, 0.4 mmol) in CH_2Cl_2 (10 mL). DDQ (1.18 g, 5.2 mmol) was dissolved in toluene–CH_2Cl_2 (1 : 1, 40 mL) and both mixtures were added simultaneously to the vigorously stirred CH_2Cl_2 (50 mL). After 15 min the reaction mixture was concentrated to 1/4 of initial volume and filtered through silica pad (CH_2Cl_2). The fluorescent band was collected, evaporated and chromatographed (DCVC, silica, CH_2Cl_2–hexanes, 1 : 1, then 3 : 1). After evaporation residue was crystallized from $CHCl_3$–hexanes to afford pure corrole (209 mg, 11%). R_f = 0.42 (CH_2Cl_2–hexanes, 3 : 1). ^{1}H NMR (500 MHz; $CDCl_3$; Me_4Si) δ (−4)–(−1.5) (br s, 3H), 5.53 (s, 2H, CH_2), 7.68 (t, 2H, J = 8 Hz, $C_{10}H_6$), 7.82, 8.07 (d + t, AA′BB′ + d, J = 8 Hz, 2 × 2H + 2H, C_6H_4 + $C_{10}H_6$), 8.54 (br d, J = 6.3 Hz, 2 + 2H, β-H + $C_{10}H_6$), 8.63 (d, J = 4.6 Hz, 2H, β-H), 8.66 (d, J = 4.6 Hz, 2H, β-H), 9.07 (d, J = 4 Hz, 2H, β-H). ESI-LR obsd 916.4 [M + H^+] ($C_{50}H_{24}F_{10}N_5O_2$). Anal. calc. for $C_{50}H_{23}F_{10}N_5O_2$: C, 65.58; H, 2.53; N, 7.65. Found: C, 65.72; H, 2.63; N, 7.54%. λ_{abs} (toluene, $\varepsilon \times 10^3$) 421 (112), 564 (17.1), 618 (10.2), 639 (8.6) nm.

10-[(Benz[*de*]isoquinoline-1,3-dion-2-yl)-*meta*-tolyl]-5,15-bis(mesityl)corrole (C1-NI1). The title compound was synthesized according to the procedure described for **C1-NI2**, starting from mesityldipyrromethane **14** (1.06 g, 4 mmol) and aldehyde **10** (602 mg, 2 mmol). The reaction mixture was concentrated, filtered through silica pad (CH_2Cl_2) and evaporated. The residue was chromatographed (DCVC, silica, CH_2Cl_2–hexanes, 1 : 1, then 3 : 1), evaporated and crystallized ($CHCl_3$–MeOH) to afford pure corrole (92 mg, 6%).

R_f = 0.39 (CH_2Cl_2–hexanes, 3 : 1). ^{1}H NMR (500 MHz; $CDCl_3$; Me_4Si) δ (−3) − (−1) (br s, 3H, NH), 1.89 (s, 6H, o-CH_3 Mes), 1.96 (s, 6H, o-CH_3 Mes), 2.57 (s, 6H, p-CH_3 Mes), 7.25 (s, 2H, Mes), 7.29 (s, 2H, Mes), 7.68 (d, J = 8 Hz, 1H, C_6H_4), 7.81 (t, 2H, J = 8 Hz, $C_{10}H_8$), 7.91 (t, 1H, J = 8 Hz, C_6H_4), 8.17 (s, 1H, C_6H_4), 8.26 (d, J = 8 Hz, 2H, $C_{10}H_6$), 8.29 (d, J = 8 Hz, 1H, C_6H_4), 8.33 (d, J = 4 Hz, 2H, β-H), 8.55 (d, J = 4.5 Hz, 2H, β-H), 8.70 (d, 2H, J = 8 Hz, $C_{10}H_6$), 8.76 (d, J = 4.5 Hz, 2H, β-H), 8.88 (d, J = 4 Hz, 2H, β-H). ESI-HR obsd 806.3482 [M + H^+], calc. exact mass 806.3489 ($C_{55}H_{44}N_5O_2$); Anal. calc. for $C_{55}H_{43}N_5O_2$: C, 81.96; H, 5.38; N, 8.69. Found: C, 81.85; H, 5.55; N, 8.85. λ_{abs} (toluene, $\varepsilon \times 10^3$) 409 (126), 428 (113), 567 (18.4), 604 (12.4), 638 (7.5) nm.

10-[(Benz[*de*]isoquinoline-1,3-dion-2-yl)-*meta*-tolyl]-5,15-bis (2,6-dichlorophenyl)corrole (C2-NI1). The title compound was synthesized according to the procedure described for **C1-NI2**, starting from 2,6-dichlorophenyldipyrromethane **15** (1.16 g, 4 mmol) and aldehyde **10** (602 mg, 2 mmol). The reaction mixture was concentrated, filtered through silica pad (CH_2Cl_2) and evaporated. The residue was chromatographed (DCVC, silica, CH_2Cl_2–hexanes, 1 : 1, then 3 : 1), evaporated and crystallized ($CHCl_3$–MeOH) to afford pure corrole (372 mg, 22%). R_f = 0.39 (CH_2Cl_2–hexanes, 3 : 1). ^{1}H NMR (500 MHz; $CDCl_3$; Me_4Si) δ (−2.5)–(−1.5) (br s, 3H, NH), 7.61 (t, 2H, 8 Hz, $C_6H_3Cl_2$), 7.67 (m, 1H, C_6H_4), 7.70–7.77 (m, 4H + 2H, $C_6H_3Cl_2$ + $C_{10}H_6$), 7.90 (t, 1H, J = 8 Hz, C_6H_4), 8.15–8.18 (m, 2H + 1H, $C_{10}H_6$ + C_6H_4), 8.28–8.31 (m, 1H, C_6H_4), 8.39 (d, J = 4 Hz, 2H, β-H), 8.58 (d, J = 4.5 Hz, 2H, β-H), 8.66 (dd, 2H, $C_{10}H_6$), 8.85 (d, J = 4.5 Hz, 2H, β-H), 8.97 (d, J = 4 Hz, 2H, β-H). EI-LR obsd 857.3 [$M^{\bullet+}$] ($C_{49}H_{28}N_5Cl_4O_2$); Anal. calc. for $C_{49}H_{27}N_5Cl_4O_2$: C, 68.74; H, 3.35; N, 8.02. Found: C, 68.59; H, 3.12; N, 7.94%. λ_{abs} (toluene, $\varepsilon \times 10^3$) 412 (117), 428 (110), 563 (19.1), 610 (12.1), 641 (6.6) nm.

10-[(Benz[*de*]isoquinoline-1,3-dion-2-yl)-*meta*-tolyl]-5,15-bis (pentafluorophenyl)corrole (C3-NI1). The title compound was synthesized according to the procedure described for **C1-NI2**, starting from pentafluorophenyldipyrromethane **16** (1.16 g, 4 mmol) and aldehyde **10** (602 mg, 2 mmol). The reaction mixture was concentrated, filtered through silica pad (CH_2Cl_2) and evaporated. The residue was chromatographed (DCVC, silica, CH_2Cl_2–hexanes, 1 : 1, then 3 : 1), evaporated and crystallized ($CHCl_3$–hexanes) gave pure corrole (404 mg, 22%). R_f = 0.39 (CH_2Cl_2–hexanes, 3 : 1).^{1}H NMR (500 MHz; $CDCl_3$; Me_4Si) δ (−4)–(−1.5) (br s, 3H), 7.63–7.66 (m, 1H, C_6H_4), 7.67 (t, 2H, J = 8 Hz, $C_{10}H_6$), 7.91 (t, J = 8 Hz, 1H, C_6H_4), 8.07 (dd, 2H, $C_{10}H_6$), 8.14 (t, J = 2 Hz, 1H, C_6H_4), 8.25–8.28 (m, 1H, C_6H_4), 8.54 (br d, J = 4 Hz, 2H, β-H), 8.57 (dd, 2H, $C_{10}H_6$), 8.75 (d, J = 4.6 Hz, 2H, β-H), 8.93 (d, J = 4.6 Hz, 2H, β-H), 9.07 (d, J = 4 Hz, 2H, β-H). ESI-LR obsd 902.3 [M + H^+] ($C_{49}H_{22}F_{10}N_5O_2$). Anal. calc. for $C_{49}H_{21}F_{10}N_5O_2$: C, 65.27; H, 2.35; N, 7.77. Found: C, 65.38; H, 2.15; N, 7.74%. λ_{abs} (toluene, $\varepsilon \times 10^3$) 423 (115), 564 (18.1), 616 (10.5), 641 (7.7) nm.

10-(4-Tolyl)-5,15-bis(mesityl)corrole (C1). Mesityldipyrromethane (1.06 g, 4.0 mmol) and 4-tolualdehyde (240 μL, 2.0 mmol) were dissolved in MeOH (400 mL). Then conc. HCl_{aq} (20 mL) in water (200 mL) was added and the resulting suspension was stirred at rt for 2 h. After extraction with $CHCl_3$ (2 × 50 mL), the organic phase was washed with water (2 × 50 mL), diluted to the volume of 250 mL, and *para*-chloranil (1.476 g, 6 mmol) was added in one portion. The resulting mixture was stirred at rt for 16 h and then solvent was removed to 1/4 of the initial volume. After filtration through silica pad (CH_2Cl_2–hexanes, 1 : 1), hydrazine (1 M solution in THF, 300 μL, 300 μmol) was added to the fractions contained desired corrole. After evaporation, the residue was chromatographed (DCVC, silica, CH_2Cl_2–hexanes, 1 : 9) and crystallized from cyclohexane–MeOH to afford pure corrole (52 mg, 4%). R_f = 0.46 (CH_2Cl_2–hexanes, 2 : 3). ^{1}H NMR (500 MHz; $CDCl_3$; Me_4Si) δ (−2.5)–(−1.5) (br s, 3H, NH), 1.92 (s, 12H, *o*-CH_3 Mes), 2.59 (s, 6H, *p*-CH_3 Mes), 2.65 (s, 3H, CH_3 Tol), 7.25 (s, 4H, Mes), 7.51, 8.03 (AA′BB′, J = 8 Hz, 2 × 2H, C_6H_4), 8.31 (d, J = 4 Hz, 2H, β-H), 8.47 (d, J = 4.5 Hz, 2H, β-H), 8.49 (d, J = 4.5 Hz, 2H, β-H), 8.87 (d, J = 4 Hz, 2H, β-H). ESI-HR obsd 625.3307 [M + H^+], calc. exact mass 625.3325 ($C_{44}H_{41}N_4$); Anal. calc. for $C_{44}H_{40}N_4$: C, 84.58; H, 6.45; N, 8.97. Found: C, 84.39; H, 6.49; N, 8.85%. λ_{abs} (toluene, $\varepsilon \times 10^3$) 409 (122), 428 (102), 568 (18.2), 605 (12.0), 639 (7.1) nm.

10-(4-Tolyl)-5,15-bis(2,6-dichlorophenyl)corrole (C2). The title compound was synthesized according to the procedure described for **C1**, starting from 2,6-dichlorophenyldipyrromethane **15** (1.16 g, 4.0 mmol) and 4-tolualdehyde (240 μL, 2.0 mmol). The reaction mixture was concentrated, filtered through silica pad (CH_2Cl_2–hexanes, 1 : 1) and evaporated. The residue was chromatographed (DCVC, silica, CH_2Cl_2–hexanes, 1 : 9) and crystallized (cyclohexane–MeOH) to afford pure corrole (162 mg, 12%). R_f = 0.43 (CH_2Cl_2–hexanes, 2 : 3). ^{1}H NMR (500 MHz; $CDCl_3$; Me_4Si) δ (−4) − (−1) (br s, 3H, NH), 2.66 (s, 3H, CH_3 Tol), 7.52, 8.05 (AA′BB′, J = 8 Hz, 2 × 2H, C_6H_4), 7.62 (t, 2H, 8 Hz, $C_6H_3Cl_2$), 7.75 (d, 8 Hz, 4H, $C_6H_3Cl_2$), 8.40 (d, J = 4 Hz, 2H, β-H), 8.51 (d, J = 4.5 Hz, 2H, β-H), 8.60 (d, J = 4.5 Hz, 2H, β-H), 8.98 (d, J = 4 Hz, 2H, β-H). ESI-HR obsd 677.0862 [M + H^+], calc. exact mass 677.0829 ($C_{38}H_{26}N_4Cl_4$); Anal. calc. for $C_{38}H_{25}N_4Cl_4 \cdot H_2O$: C, 65.53; H, 3.76; N, 8.04. Found: C, 65.50; H, 3.57; N, 7.90%. λ_{abs} (toluene, $\varepsilon \times 10^3$) 412 (120), 428 (106), 563 (19.1), 612 (12.1), 641 (7.0) nm.

Spectroscopy and photophysics

Spectrophotometric grade toluene at 295 K and at 77 K was used without further purification. Standard 10 mm fluorescence cells were used at 295 K whereas experiments at 77 K made use of capillary tubes in a home made quartz Dewar filled with liquid nitrogen. Due to geometrical conditions at 77 K the absolute quantum yield cannot be determined. If not otherwise specified, solutions were air-equilibrated. A Perkin-Elmer Lambda 5 UV/Vis spectrophotometer and a Spex Fluorolog II spectrofluorimeter were used to acquire absorption and emission spectra. Reported luminescence spectra are uncorrected, unless otherwise specified. Emission quantum yields were determined after correction for the photomultiplier response, with reference to air-equilibrated toluene solutions of TPP with a Φ_{fl} = 0.11[40] or to quinine sulfate in 1N sulfuric

acid with $\Phi_{fl} = 0.546$.[41] Luminescence lifetimes in the nanosecond range were obtained with an IBH single photon counting equipment with excitation at 560 nm from a pulsed diode source (resolution 0.3 ns). For determination of emission lifetimes in the picosecond range an apparatus based on a Nd:YAG laser (35 ps pulse duration, 355 nm, 1.5 mJ) and a Streak Camera with overall resolution of 10 ps was used.[42] Attempts to determine the CS spectra and lifetimes in the picosecond range were performed by a pump–probe apparatus with 30 ps resolution based on a Nd-YAG laser (355 nm or 532 nm, 3 mJ, 35 ps pulse duration, 10 Hz) and an optical multichannel analizer (Roper Scientific, Acton Research, Acton MA), further details on the experimental set-up were reported previously.[43] The stability of solutions was carefully checked after each experiment by spectrophotometric control and, unless otherwise specified, the samples were perfectly stable. Experimental uncertainties are estimated to be within 10% for lifetime determination, 15% for quantum yields, 20% for molar absorption coefficients and 3 nm for emission and absorption peaks. The temperature of operation was 295 K except otherwise stated. Computation of the integral overlaps and of the rate for the energy transfer processes according to Förster and Dexter mechanism were performed with the use of Matlab 5.2.[44]

Electrochemistry

Benzonitrile (PhCN, 99.9% CHROMASOLV from Sigma-Aldrich) was distilled over P_2O_5 under vacuum prior to use. Vacuum-dried tetra-*n*-butylammonium perchlorate (TBAP, electrochemical grade from Fluka) was used as supporting electrolyte ($c = 0.1$ M). The concentration of reactants was 0.5 mM.

Cyclic voltammetry was carried out with a EG&G PAR 273A potentiostat controlled by a PC computer by means of the software M270 from PAR. The positive feedback method of iR compensation was applied. A three-electrode cell was used consisting of a platinum-disk working electrode (1.5 mm diameter), a platinum counter electrode and a saturated calomel reference electrode (SCE). All potentials are referred against SCE. The solution was deoxygenated with argon and a blanket of gas was maintained over the solution surface during measurements.

Conclusions

Our studies have clearly documented the ability of the dipyrromethane + aldehyde strategy to assemble corrole skeletons with more elaborated substituents. By using this sequence, corrole dyads could be prepared from commercially available reagents in just 2–5 steps. Respective aldehydes were generated in simple synthetic pathways.

The dyads have been spectroscopically and photophysical characterized and display an excellent stability in toluene. When the system is excited in the naphthalene imide manifold, the ensuing singlet excited state has enough energy to display intramolecular reactivity. Competitive energy and electron transfer have been evidenced, the relative weight of the two processes being determined by the driving force for charge separation. The energy transfer efficiency decreases from 100% in the dyads containing the corrole more difficult to oxidize to 65% and 15% in the dyads containing corrole with progressively lower oxidation potentials whereas electron transfer efficiency follows the reverse pattern. Energy transfer is discussed in the frame of current theories; a dipole–dipole mechanism could explain the process in dyads containing the imide **NI2**, though we cannot exclude a contribution by an electron exchange mechanism. A large contribution by an electron exchange mechanism is proposed in dyads containing the non emitting imide **NI1**. Excitation in the corrole manifold yields an excited state which does not display any intramolecular reactivity due to its low energy.

These systems represent one of the few examples of photostable corrole based arrays exhibiting intramolecular photoinduced energy transfer[13b,14e] and the first example of corrole-based molecular ensembles displaying photoinduced electron transfer. This confirms the suitability of corrole unit as a building block for molecular architectures displaying functionality driven by light energy.

Acknowledgements

We thank Volkswagen Foundation, Polish Ministry of Science and Education, CNR of Italy (Project: Componenti molecolari e supramolecolari o macromolecolari con proprietà fotoniche ed optoelettroniche) and Ministero dell'Istruzione, dell'Universita' e della Ricerca of Italy (FIRB, RBNE019H9K) for financial support.

References

1 (*a*) G. McDermott, S. M. Prince, A. A. Freer, A. M. Hawthornthwaite-Lawless, M. Z. Papiz, R. J. Cogdell and N. W. Isaacs, *Nature*, 1995, **374**, 517–520; (*b*) A. W. Roszak, T. D. Howard, J. Southall, A. T. Gardiner, C. J. Law, N. W. Isaacs and R. J. Cogdell, *Science*, 2003, **302**, 1969–1972; (*c*) A. Ben-Shem, F. Frolow and N. Nelson, *Nature*, 2003, **426**, 630–635; (*d*) D. Gust, T. A. Moore and A. L. Moore, *Acc. Chem. Res.*, 2001, **34**, 40–48; (*e*) M. R. Wasielewski, *Chem. Rev.*, 1992, **92**, 435–461; (*f*) J. H. Alstrum-Avecedo, M. K. Brennaman and T. J. Meyer, *Inorg. Chem.*, 2005, **44**, 6802–6827; (*g*) M. R. Wasielewski, *J. Org. Chem.*, 2006, **71**, 5051–5066.

2 (*a*) S. L. Gould, G. Kodis, P. A. Liddell, R. E. Palacios, A. Brune, D. Gust, T. A. Moore and A. L. Moore, *Tetrahedron*, 2006, **62**, 2074–2096; (*b*) R. H. Goldsmith, L. E. Sinks, R. F. Kelley, L. J. Betzen, W. Liu, E. A. Weiss, M. A. Ratner and M. R. Wasielewski, *Proc. Natl. Acad. Sci. U. S. A.*, 2005, **102**, 3540–3545.

3 (*a*) D. Gust and T. A. Moore, in *The Porphyrin Handbook*, ed. K. M. Kadish, K. M. Smith and R. Guilard, Academic Press, New York, 2000, vol. 8, pp. 153–190; (*b*) D. Holten, D. F. Bocian and J. S. Lindsey, *Acc. Chem. Res.*, 2002, **35**, 57–69; (*c*) H. Imahori, *J. Phys. Chem. B*, 2004, **108**, 6130–6143; (*d*) Y. Kobuke and K. Ogawa, *Bull. Chem. Soc. Jpn.*, 2003, **76**, 689–708; (*e*) K. Kilså, J. Kajanus, S. Larsson, A. N. Macpherson, J. Mårtensson and B. Albinsson, *Chem.–Eur. J.*, 2001, **7**, 2122–2133.

4 (*a*) S. G. DiMagno, V. S.-Y. Lin and M. J. Therien, *J. Org. Chem.*, 1993, **58**, 5983–5993; (*b*) M. O. Senge and I. Bischoff, *Eur. J. Org. Chem.*, 2001, 1735–1751; (*c*) J. S. Lindsey, in *The Porphyrin Handbook*, ed. K. M. Kadish, K. M. Smith and R. Guilard, Academic Press, New York, 2000, vol. 1, pp. 45–118; (*d*) M. O. Senge and J. Richter, *J. Porphyrins Phthalocyanines*, 2004, **8**, 934–953; (*e*) K. M. Smith and M. G. H. Vicente, in *Science of Synthesis*, ed. S. M. Weinreb, Georg Thieme Verlag, Stuttgart, New York, 2004, pp. 1081–1235.

5 K. Kalyanasundaram, *Photochemistry of Polypyridine and Porphyrin Complexes*, Academic Press, London, 1992, part III, pp. 369–603, and references therein.

6 (*a*) X. Li, L. E. Sinks, B. Rybtchinski and M. R. Wasielewski, *J. Am. Chem. Soc*., 2004, **126**, 10810–10811; (*b*) D. M. Guldi, I. Zilbermann, A. Gouloumis, P. Vazquez and T. Torres, *J. Phys. Chem. B*, 2004, **108**, 18485–18494; (*c*) D. M. Guldi and H. Imahori, *J. Porphyrins Phthalocyanines*, 2004, **8**, 976–983.

7 (*a*) D. Gonzalez-Rodriguez, T. Torres, D. M. Guldi, J. Rivera, M. A. Herranz and L. Echegoyen, *J. Am. Chem. Soc*., 2004, **126**, 6301–6313; (*b*) D. Gonzalez-Rodriguez, C. G. Claessens, T. Torres, S. G. Liu, L. Echegoyen, N. Vila and S. Nonell, *Chem.–Eur. J*., 2005, **11**, 3881–3893.

8 (*a*) T. S. Balaban, H. R. Tamiaki and A. Holzwarth, 'Supramolecular Dye Chemistry', , in *Topics in Current Chemistry*, ed. F. Würthner, , Springer, Berlin, 2005, vol. 258, pp. 1–38; (*b*) T. S. Balaban, *Acc. Chem. Res*., 2005, **38**, 612–623.

9 (*a*) V. Huber, M. Katterle, M. Lysetska and F. Würthner, *Angew. Chem., Int. Ed*., 2005, **44**, 3147–3151; (*b*) S. Sasaki, T. Mizoguchi and H. Tamiaki, *Tetrahedron*, 2005, **61**, 8041–8048; (*c*) R. F. Kelley, M. J. Tauber and M. R. Wasielewski, *J. Am. Chem. Soc*., 2006, **128**, 4779–4791; (*d*) C. Röger, M. G. Müller, M. Lysetska, Y. Miloslavina, A. R. Holzwarth and F. Würthner, *J. Am. Chem. Soc*., 2006, **128**, 6542–6543.

10 (*a*) N. Mataga, S. Taniguchi, H. Chosrowjan, A. Osuka and N. Yoshida, *Photochem. Photobiol. Sci*., 2003, **2**, 493–500; (*b*) I. W. Hwang, T. Kamada, T. K. Ahn, D. M. Ko, T. Nakamura, A. Tsuda, A. Osuka and D. Kim, *J. Am. Chem. Soc*., 2004, **126**, 16187–16198; (*c*) I. W. Hwang, N. Aratani, A. Osuka and D. Kim, *Bull. Korean Chem. Soc*., 2005, **26**, 19–31.

11 (*a*) R. Paolesse, in *The Porphyrin Handbook*, ed. K. M. Kadish, K. M. Smith and R. Guilard, Academic Press, New York, 2000, vol. 2, pp. 201–232; (*b*) D. T. Gryko, *Eur. J. Org. Chem*., 2002, 1735–1742; (*c*) R. Guilard, J.-M. Barbe, C. Stern and K. M. Kadish, in *The Porphyrin Handbook*, ed. K. M. Kadish, K. M. Smith and R. Guilard, Elsevier Science (U. S. A.), vol. 18, pp. 303–351; (*d*) D. T. Gryko, J. P. Fox and D. P. Goldebrg, *J. Porphyrins Phthalocyanines*, 2004, **8**, 1091–1105; (*e*) S. Nardis, D. Monti and R. Paolesse, *Mini-Rev. Org. Chem*., 2005, **2**, 355–372.

12 (*a*) B. Koszarna and D. T. Gryko, *J. Org. Chem*., 2006, **71**, 3707–3717; (*b*) J.-M. Barbe, G. Canard, S. Brandès and R. Guilard, *Eur. J. Org. Chem*., 2005, 4601–4611.

13 (*a*) B. Ventura, A. Degli Esposti, B. Koszarna, D. T. Gryko and L. Flamigni, *New J. Chem*., 2005, **29**, 1559–1566; (*b*) L. Flamigni, B. Ventura, M. Tasior and D. T. Gryko, *Inorg. Chim. Acta*, 2006DOI: 10.1016/j.ica.2006.03.021.

14 (*a*) J. Bendix, I. J. Dmochowski, H. B. Gray, A. Mahammed, L. Simkhovic and Z. Gross, *Angew. Chem., Int. Ed*., 2000, **39**, 4048–4051; (*b*) R. Paolesse, A. Marini, S. Nardis, A. Froiio, F. Mandoj, D. J. Nurco, L. Prodi, M. Montalti and K. M. Smith, *J. Porphyrins Phthalocyanines*, 2003, **7**, 25–36; (*c*) J. J. Weaver, K. Sorasaenee, M. Sheikh, R. Goldschmidt, E. Tkachenko, Z. Gross and H. B. Gray, *J. Porphyrins Phthalocyanines*, 2004, **8**, 76–81; (*d*) T. Ding, E. A. Alemán, D. A. Mordarelli and C. J. Ziegler, *J. Phys. Chem. A*, 2005, **109**, 7411–7417; (*e*) J. Poulin, C. Stern, R. Guilard and P. D. Harvey, *Photochem. Photobiol*., 2006, **82**, 171–176; (*f*) R. Paolesse, F. Sagone, A. Macagnano, T. Boschi, L. Prodi, M. Montalti, N. Zaccheroni, F. Bolletta and K. M. Smith, *J. Porphyrins Phthalocyanines*, 1999, **3**, 364–370.

15 (*a*) T. Van der Boom, R. T. Hayes, Y. Zhao, P. J. Bushard, E. A. Weiss and M. R. Wasielewski, *J. Am. Chem. Soc*., 2002, **124**, 9582–9590; (*b*) K. Tomizaki, R. S. Loewe, C. Kirmaier, J. K. Scwartz, J. L. Retsek, D. F. Bocian, D. Holten and J. S. Lindsey, *J. Org. Chem*., 2002, **67**, 6519–6534; (*c*) K. Okamoto, Y. Mori, H. Yamada, H. Imahori and S. Fukuzumi, *Chem.–Eur. J*., 2004, **10**, 474–483.

16 (*a*) V. Wintgens, P. Valat, J. Kossanyi, L. Biczok, A. Demeter and T. Berces, *J. Chem. Soc., Faraday Trans*., 1994, **90**, 411–421; (*b*) A. Samanta, B. Ramachandram and G. Saroja, *J. Photochem. Photobiol., A*, 1996, **101**, 29–32.

17 (*a*) I. Saito, *Pure Appl. Chem*., 1992, **64**, 1305–1310; (*b*) M. Licchelli, A. O. Biroli, A. Poggi, D. Sacchi, C. Sangermani and M. Zema, *Dalton Trans*., 2003, 4537–4545.

18 (*a*) Q. Tan, D. Kaciaukas, S. Lin, S. Stone, A. L. Moore, T. A. Moore and D. Gust, *J. Phys. Chem. B*, 1997, **101**, 5214–5223; (*b*) D. W. Cho, M. Fujitsuka, A. Sugimoto, U. C. Yoon, P. S. Mariano and T. Majima, *J. Phys. Chem. B*, 2006, **110**, 11062–11068; (*c*) T. P. Le, J. E. Rogers and L. A. Kelly, *J. Phys. Chem. A*, 2000, **104**, 6778–6785; (*d*) S. Abad, M. Kluciar, M. A. Miranda and U. Pischel, *J. Org. Chem*., 2005, **70**, 10565–10568.

19 (*a*) W. H. Zhu, H. Tian, E. Q. Gao, M. Z. Yang and K. Muellen, *Chem. Lett*., 2000, **7**, 778–779; (*b*) H. Tian, P. H. Liu, W. H. Zhu, E. Q. Gao, W. A. Da-Jun and S. M. Cai, *J. Mater. Chem*., 2000, **10**, 2708–2715; (*c*) A. S. Lukas, P. J. Bushard and M. R. Wasielewski, *J. Am. Chem. Soc*., 2001, **123**, 2440–2441; (*d*) T. Gunlaugsson, T. C. Lee and R. Parkesh, *Org. Biomol. Chem*., 2003, **1**, 3265–3267.

20 R. W. Middleton, J. Parrick, E. D. Clarke and P. Wardman, *J. Heterocycl. Chem*., 1986, **23**, 849–855.

21 (*a*) D. T. Gryko and K. Jadach, *J. Org. Chem*., 2001, **66**, 4267–4275; (*b*) D. T. Gryko and K. E Piechota, *J. Porphyrins Phthalocyanines*, 2002, **6**, 81–97; (*c*) D. T. Gryko and B. Koszarna, *Org. Biomol. Chem*., 2003, **1**, 350–357; (*d*) D. T. Gryko and B. Koszarna, *Synthesis*, 2004, 2205–2209.

22 W. Gelmo, *J. Prakt. Chem*., 1913, **88**, 818–831.

23 H. Imahori, K. Tamaki, Y. Araki, T. Hasobe, O. Ito, A. Shimomura, S. Kundu, T. Okada, Y. Sakata and S. Fukuzumi, *J. Phys. Chem. A*, 2002, **106**, 2803–2814.

24 J. Shen, J. Shao, Z. Ou, W. E, B. Koszarna, D. T. Gryko and K. M. Kadish, *Inorg. Chem*., 2006, **45**, 2251–2265.

25 P. Valat, V. Wintgens, J. Kossanyi, L. Biczók, A. Demeter and T. Bérces, *J. Am. Chem. Soc*., 1992, **114**, 946–953.

26 S. K. Lee, Y. Zu, A. Herrmann, Y. Geerts, K. Müllen and A. J. Bard, *J. Am. Chem. Soc*., 1999, **121**, 3513–3520.

27 J. E. Rogers, S. J. Weiss and L. A. Kelly, *J. Am. Chem. Soc*., 2000, **122**, 427–436.

28 Y. O. Su, K.-Y. Chiu, T.-H. Lin, S.-J. Shieh and S.-C. Lin, *J. Org. Chem*., 2005, **70**, 4323–4331.

29 M. J. Ahrens, M. J. Tauber and M. R. Wasielewski, *J. Org. Chem*., 2006, **71**, 2107–2114.

30 A. Demeter, L. Biczók, T. Bérces, V. Wintgens, P. Valat and J. Kossanyi, *J. Phys. Chem*., 1993, **97**, 3217–3224.

31 A. Weller, *Z. Phys. Chem., Neue Folge*, 1982, **133**, 93–98.

32 (*a*) S. R. Greenfield, W. A. Svec, D. Gosztola and M. R. Wasielewski, *J. Am. Chem. Soc*., 1996, **118**, 6767–6777; (*b*) L. Flamigni, B. Ventura, C.-C. You, C. Hippius and F. Würthner, *J. Phys. Chem. C*, DOI: 10.1021/jp065394g.

33 Th. Förster, *Discuss. Faraday Soc*., 1959, **27**, 7–17.

34 D. L. Dexter, *J. Chem. Phys*., 1953, **21**, 836–850.

35 D. S. Pedersen and C. Rosenbohm, *Synthesis*, 2001, 2431–2434.

36 A. D. Andricopulo, L. A. Mueller, V. C. Filho, G. S. Cani, J. F. Roos, R. Correa, A. R. S. Santos, R. J. Nunes and R. A. Yunes, *Farmaco*, 2000, **55**, 319–321.

37 (*a*) B. J. Littler, M. A. Miller, C. H. Hung, R. W. Wagner, D. F. O'Shea, P. D. Boyle and J. S. Lindsey, *J. Org. Chem*., 1999, **64**, 1391–1396; (*b*) J. K. Laha, S. Dhanalekshmi, M. Taniguchi, A. Ambroise and J. S. Lindsey, *Org. Process Res. Dev*., 2003, **7**, 799–812.

38 H. Cao, V. Chang, R. Hernandez and M. D. Heagy, *J. Org. Chem*., 2005, **70**, 4929–4934.

39 T. Sakamoto and C. Pac, *J. Org. Chem*., 2001, **66**, 94–98.

40 P. G. Seybold and M. J. Gouterman, *J. Mol. Spectrosc*., 1969, **31**, 1–13.

41 D. F. Eaton, *Pure Appl. Chem*., 1988, **60**, 1107–1114.

42 L. Flamigni, *J. Phys. Chem*., 1993, **97**, 9566–9572.

43 L. Flamigni, A. M. Talarico, S. Serroni, F. Puntoriero, M. J. Gunter, M. R. Johnston and T. P. Jeynes, *Chem.–Eur. J*., 2003, **9**, 2649–2659.

44 *Matlab 5.2*, The MathWorks Inc., Natik, MA 01760, USA, 1998.